Islamic Azad University

Journal of

Optoelectronical Nanostructures

Summer 2019 / Vol. 4, No. 3

Thermodynamic study of (pb^{2+}) removal by adsorption onto modified magnetic Graphene Oxide with Chitosan and Cysteine

Ghazaleh Ramezani[*,1], Bizhan Honarvar[1], Masoomeh Emadi[2]

[1] Department of Chemical Engineering, Marvdasht Branch, Islamic Azad University,Marvdasht, Iran

[2] Department of Chemistry, Marvdasht Branch, Islamic Azad University, Marvdasht, Iran

(Received 23 Jun. 2019; Revised 22 Jul. 2019; Accepted 13 Aug. 2019; Published 15 Sep. 2019)

Abstract: A new modified magnetic Graphene Oxide with Chitosan and Cysteine was synthesized for removing Pb^{2+} ions from aqueous solution. The properties of this adsorbent were characterized by Field Emission Scanning Electron Microscopy (FE-SEM), Vibrating Sample Magnetometer (VSM) and Energy Dispersive Analysis System of X-ray (EDAX). Physicochemical parameters such as effect of pH, contact time, adsorbent dosage and initial concentration of Pb^{2+} was also studied. The results showed that the maximum capacity of absorbent in Lead ions adsorption (at Equilibrium concentration of 120 ppm) occurred at $pH_{Optimum}$= 5.75, $t_{Optimum}$= 30 min and adsorbent 85.4 mg/g dosage=0.1 gr. Maximum empirical adsorption capacity (q_{max}) was calculated 85.4 mg/g. The thermodynamic parameters (ΔH^o, ΔG^o and ΔS^o) showed that the adsorption process of Pb^{2+} on modified magnetic Graphene Oxide with Chitosan and Cysteine was endothermic and spontaneous. Removal percentage was reduced to 15% after five stages of Sorption/desorption studies. So, modified magnetic Graphene Oxide with Chitosan and Cysteine can be used as a complementary process for removal of Pb^{2+} ions from water and wastewater.

Keywords: Magnetic Graphene Oxide, Surface modification, Nanoparticles, Removal of lead, Adsorption thermodynamics

1. INTRODUCTION

Lead is one of the most toxic metal ions and it's found in +2 oxidation state (Pb^{2+}) in the inorganic form. Its presence in drinking water resources, can damage to the brain, blood composition, liver, kidney, nervous and reproductive system [1,2]. Removal of lead ions from aquatic systems has attracted the

* Corresponding author. Email: ghazaleh_ramezani_70@yahoo.com

attention of researchers. The limit of Lead concentration in drinking water specified 10 ppb from the World Health Organization [3].

Many processes were developed to treat water pollution with metal ions, such as membrane separation process, chemical precipitation, ion exchange and adsorption [4]. Among these commonly methods, adsorption processes are more popular than the others due to their high removal efficiency and the simplicity of the purification process [5]. Efficiency of adsorption processes have directly depended on the kind of adsorbent.

In recent decades, nanomaterials based on carbon allotropes especially Graphene based materials, such as Graphene Oxide (GO) and Reduced Graphene Oxide (R-GO) have been used as efficient and affordable adsorbents in adsorption processes [6- 8]. Unique properties of Graphene like; mechanical strength, great flexibility, good solubility and particularly large specific surface area are reasons that cause Graphene, as the famous material of the 21st century, to be used in synthesis various nanocomposites [9,10]. Among the various Graphene structures, GO is a very oxidative form of Graphene [11]. GO has lots of oxygenated functional groups like; Hydroxyl (-OH) and Epoxy on the surface of its carbons plates and, Carboxyl (-COOH) and Carbonyl (C=O) groups, at the edges of the plates [12, 13]. These functional groups have been able to remove different substances from aqueous solutions like metal ions and dyes [14,15]. But on the other hand, GO sheets have a tendency to accumulate in aqueous solutions and make Graphite sheets again. Accumulation of them causes remarkable decrease in specific surface area. In addition, separation of Graphene and GO after adsorption process needs high-speed centrifuges and in some cases, they can cause secondary water pollution [16].

Suspended absorbent particles can be separated from water by using the magnetic properties of Fe_3O_4 nanoparticles in the absorbents structure and creating an external magnetic field. These methods are called Magnetic Separation Techniques (MST). MST techniques are able to decrease secondary water pollution tangibly [17]. Fe_3O_4 nanoparticles can increase the specific surface area of absorbents. To prevent from oxidizing of Fe_3O_4 nanoparticles when in contact with the atmosphere and increasing the stability and selectivity of these particles, many researchers attempted to modify the surface of these nanoparticles with polymers [18]. Chitosan (Chi) as a natural polysaccharide, non-toxic substance, antibacterial and affordable polymer, with having many functional groups of Amino (-NH_2) and Hydroxyl (-OH) in its structure, can be a good choice for surface modification [19, 20]. Chi is able to remove metal ions via adsorption, chelate and ion exchange by using its active ligands [21].

In this study, in addition to the use of MST technique and surface modification of magnetic Graphene Oxide with Chitosan (GO/Fe_3O_4/Chi),

amino acid Cysteine (Cys) was used to improve performance of the absorbent. Cys has thiol (-SH) agent in its structure [22], so it can bond well with metal ions such as: Zinc, Lead, Copper and Cadmium [23-25]. The characterization of modified magnetic Graphene Oxide with Chitosan and Cysteine ($GO/Fe_3O_4/Chi/Cys$) was analyzed carefully by Field Emission Scanning Electron Microscope (FE-SEM), Vibrating Sample Magnetometer (VSM) and energy dispersive analysis system of X-ray (EDAX). $GO/Fe_3O_4/Chi/Cys$ was used to remove Lead ions from synthetic wastewater in a batch system. The influence of the effective parameters like; pH, contact time, adsorbent dosage and initial concentration of Lead solution on the adsorption investigated and optimized. Finally, thermodynamic parameters (ΔH^o, ΔG^o and ΔS^o) were calculated and the regeneration study of adsorbent was investigated.

2. EXPERIMENTAL METHODS

2.1. MATERIALS

Natural Graphite powder, pure Ethanol, Chlorodic acid, Glacial Acetic acid, Ferrous Chloride tetrahydrate ($FeCl_2.4H_2O$), Ferrous Chloride hexahydrate ($FeCl_3.6H_2O$), Sodium Hydroxide, Pyridine, Lead Nitrate salt and L-Cystein were purchased from Merck (Darmstadt, Germany). Acetic acid, Glutaraldehyde, Sulfuric acid, Sodium nitrate, Potassium permanganate, Hydrogen peroxide and Ethanol were obtained from Sigma-Aldrich, Germany. Ammonia (25% by weight) with a molecular weight of 17.03 gr/mol was bought from Arvin Chem Co. Chitosan powder (CS, Mw 1.3 × 105 Da, 90% deacetylation) was supplied by Sinopharm Chemical Reagent Ltd (Shanghai, China).

2.2. Preparation of $GO/Fe_3O_4/Chi/Cys$ nanocomposite

2.2.1. PREPARATION OF GO/Fe_3O_4

Graphene Oxide was prepared via modified Hummers method. Graphite powder (20 gr) and Sodium nitrate (40 gr) were added to Sulfuric acid solution (500 ml) and the mixture was stirred at $0^{\circ}C$. Potassium permanganate (120 gr) was added to the mixture gradually. The mixed solution was diluted with double distilled water until it reached the bright Brown color. Hydrogen peroxide solution (150 ml, 30% wt.) was added to the resultant solution. For removing residual metal ions and getting to neutral pH, the mixture was washed and centrifuged several times with Hydrogen chloride solution (10% v) and double distilled water. The synthesized Graphene Oxide was kept wet for the next surface modification step.

$FeCl_3.6H_2O$ (150 gr) and $FeCl_2.4H_2O$ (60 gr) were dispersed in Hydrogen chloride solution (100 ml, 0.4 M). Iron solution (with molar ratios between Fe^{2+}

and Fe^{3+} 2:1) was added to Graphene Oxide solution (1100 ml). The mixture was stirred for 2 hours and then added immediately to Ammonia solution (1500 ml, 0.7 M). Ammonia solution was degasified farther with Argon gas for 15 minutes. The reaction system was mixed at 60°C for 2 hours and then stirred at room temperature for 12 hours. The Black precipitate was collected and washed with double distilled water until its pH reached about ~7. GO/ Fe_3O_4 was kept wet for the next step.

2.2.2. PREPARATION OF GO/ Fe_3O_4/ Chi

Chitosan (2.2 gr) was dispersed in Acetic acid solution (100 ml, 4% v) and then added to GO/ Fe_3O_4. Glutardialdehyde (4 ml, 25% wt.) was added and the reaction mixture was mixed. Sodium Hydroxide (2M) was added to achieve to neutral pH. The resultant solution was stirred and heated for 1 hour at 60°C and was stirred for 24 hours at room temperature. the desired mixture was filtered and washed with double distilled water. The product was dried for 48 hours at 60°C and crushed with ceramic mill.

2.2.3. PREPARATION OF GO/ Fe_3O_4/Chi/CYS

Glutaraldehyde (2 ml, 25% wt.) and Glacial Acetic Acid (1 ml) were suspended in pure Ethanol (30 ml). The mixture was stirred and heated at 80°C. L-Cystein (1.21 gr) was added to pure Ethanol (10 ml) and heated at 120°C. Two solutions were combined and were mixed well. The resultant mixture was kept for 24 hours under reflux condition in an oil bath at 120°C. The green precipitate was filtered and washed with hot Ethanol (50 ml) and was dried.

Dried precipitate (1 gr), Ethanol (100 ml), Glutaraldehyde (2 ml) and Pyridine (0.1 ml) were mixed and added to magnetic Graphene Oxide modified with Chitosan (GO/Fe_3O_4/Chi). Reaction mixture was kept for 48 hours at 120°C. The result solution was filtered and washed with hot Ethanol and double distilled water. Final product was dried and crushed with ceramic mill.

3.2. BATCH ADSORPTION EXPERIMENTS

All batch experiments were performed at room temperature, in a conical flask containing 40 ml Lead solutions with determined initial concentration between 10 and 400 $mg.L^{-1}$, and specified pH intervals from 1 to 6. To begin the adsorption process of Lead in flask, the amount of 0.015 to 0.3 gr of GO/Fe_3O_4/Chi/Cys was added to the Lead solution, and then the mixture shook by using a shaker (Werke, model KS 501) with a constant shaking speed of 150 rpm. After achiving to the designed removal time (in the range from 3 to 180 min), GO/Fe_3O_4/Chi/Cys dispersed in water solution was seprated quickly by applying a strong external magnetic field.

Residual concentration of Lead was determined with linear calibration curves of atomic absorption spectrometer (Varian AA220 model).

The adsorption capacity of GO/Fe_3O_4/Chi/Cys (q_e in mg/gr) and removal efficiency (% R) were calculated as:

$$q_e = \left[\frac{C_0 - C_e}{m}\right] \times v \quad (1)$$

And:

$$\%R = \left[\frac{C_0 - C_e}{C_0}\right] \times 100 \quad (2)$$

In both above equations; C_0 and C_e ($mg.L^{-1}$) show the initial concentration (at time=0) and equilibrium concentration of lead in water solutions, respectively. V is the volume of the sample solution in liter and m is the adsorbent mass in gr [26, 27].

4.2. THERMODYNAMIC STUDIES

In order to calculation of thermodynamic parameters, the effect of temperature on the lead adsorption process was investigated. The temperature of lead solutions (40 ml at equilibrium concentration =250ppm) was adjusted to different values (269, 274, 295, 315 and 346 ^oK) by using a cold water bath and a heater. The adsorption experiments occurred at $pH_{Optimum}$=5.75, $t_{Optimum}$=30min and adsorbent dosage=0.1 gr. Residual concentration of Lead in samples was determined with linear calibration curves of atomic absorption spectrometer.

5.2. REUSABILITY STUDIES

The ability of an adsorbent to be regenerated and reused in a cyclic manner is important for practical applications. In order to regenerate the adsorbent, the desorption process was performed by stirring of a certain amount of the adsorbent (0.1 g) with a certain volume (40 ml) of the pb^{2+} solution (250 ppm) at room temperature for 30 min. Then, the adsorbent was filtered, washed with 20 ml distilled water thoroughly. This action was repeated three times. After that, 20 ml HCl solution (0.1 M) was added to the adsorbent. The adsorbent was stirred for 10 min and filtered. GO/Fe_3O_4/Chi/Cys was washed several times with distilled water and dried at 22 °C. The reusability of the adsorbent was determined by performing the adsorption/desorption process in five repeated cycles with the same adsorbent.

3. RESULTS AND DISCUSSION

3.1. CHARACTERIZATION OF GO/ Fe_3O_4/Chi/CYS

3.1.1. FIELD EMISSION SCANNING ELECTRON MICROSCOPE (FE-SEM) ANALYSIS

In order to study the morphology and structure of synthesized nanocomposite at different stages of surface modification, Field Emission Scanning Electron Microscope (FE-SEM) analysis was investigated. For this purpose, FE-SEM instrument (the SIGMA VP model) was used in 25 kv and the results was shown in Fig.1. As seen in Fig.1.a; Graphene Oxide s sheets had a completely porous and irregular structure with particle size smaller than 200 nm. According to Fig.1.b, Fe_3O_4 nanoparticles with the size of about 60 nm were taken placed successfully on the Graphene Oxide s sheets. Fig.1.c represents a thin coating of Chitosan at the adsorbent surface which causes a fundamental change in the adsorbent morphological structure. At this stage; the adsorbents surface seems relatively rough. According to Fig.1.d the final structure of the nanocomposite is non-uniform and heterogeneous.

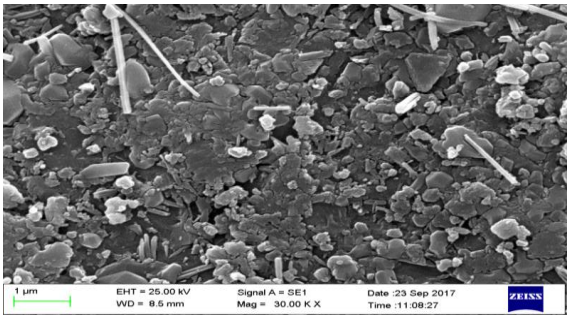

Fig.1.a. FE-SEM image of GO

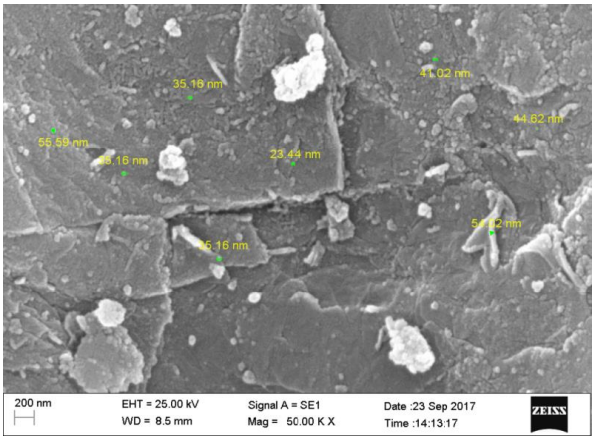

Fig.1.b. FE-SEM image of GO/ Fe_3O_4

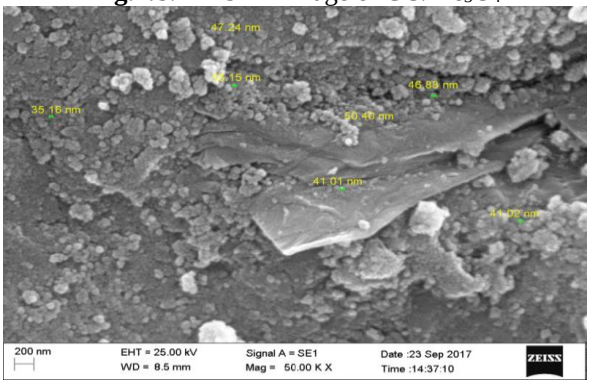

Fig.1.c. FE-SEM image of GO/ Fe_3O_4/Chi

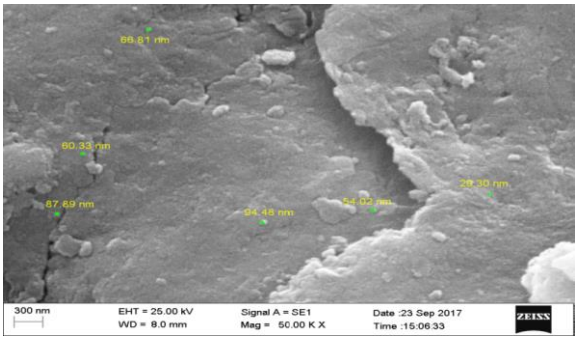

Fig.1.d. FE-SEM image of GO/Fe_3O_4/Chi/Cys

Fig.1. FE-SEM images of GO/Fe_3O_4/Chi/Cys at different stages of surface modification

3.1.2. VIBRATING SAMPLE MANETOMETER (VSM) ANALYSIS

The magnetic hysteresis loops of GO/Fe_3O_4 and GO/Fe_3O_4/Chi/Cys were recorded by a SQUID magnetometer in Fig.2. As can be seen; two curves were S-like and were near zero coercivity. The results show the absorbents have had a superparamagnetic property in such a way that by removing the external magnetic field, the magnetic property does not remain in the absorbents. The saturation magnetization (MS) values of GO/Fe_3O_4 and GO/Fe_3O_4/Chi/Cys were measured 6.94 (emu⁄gr) and 6.45 (emu⁄gr) in 15KQ, respectively. This decrease in the saturation magnetization value is due to a decrease in the ratio of Fe_3O_4 nanoparticles in GO/Fe_3O_4/Chi/Cys (with surface modification by Chitosan and Cysteine) relative to GO/Fe_3O_4. Anyway the experimental observations showed the magnetic property of final nanocomposite was high enough for relatively fast magnetic separation.

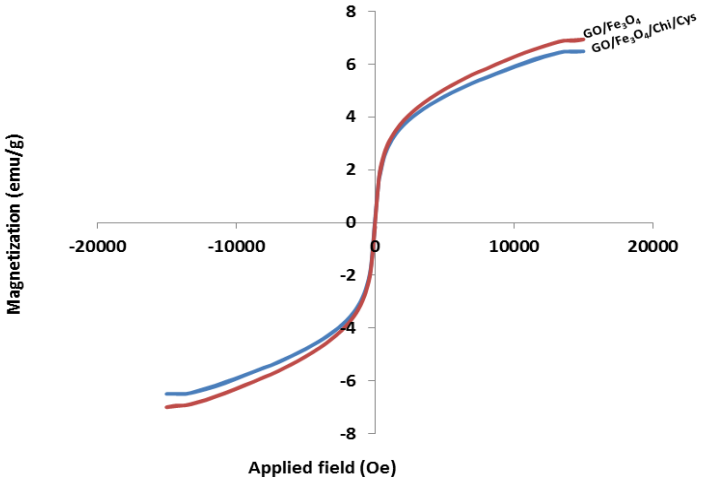

Fig.2. Magnetization saturation curve of GO/Fe3O4 and GO/Fe3O4/Chi/Cys

3.1.3. EDX ANALYSIS

Before adsorption process, the sample of GO/Fe_3O_4/Chi/Cys was subjected to EDX analysis as shown in Fig. 3. Table 1 shows the existence of O, Fe and S in sample of GO/Fe_3O_4/Chi/Cys adsorbent. The presence of these elements indicates successful modification of the adsorbent according to the aim of this work.

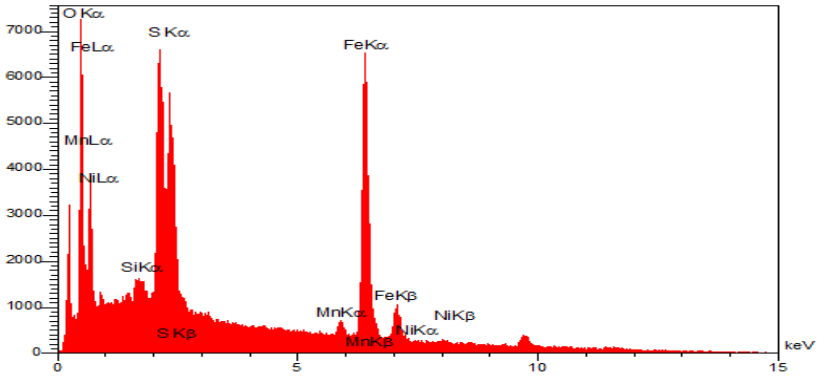

Fig.3. EDX spectra of GO/Fe_3O_4/Chi/Cys before adsorption

Table.1. The chemical composition of GO/Fe_3O_4/Chi/Cys before loaded with Pb^{2+}

Elt	W%
C	17.98
O	28.20
Si	2.32
S	14.98
Mn	1.63
Fe	31.82
Ni	3.07
	100.00

3.2. INVESTIGATION AND OPTIMIZATION OF THE EFFECTIVE PARAMETERS ON THE ADSORPTION

3.2.1. EFFECT OF THE PH VALUE

Fig.4.a shows the percentage of formed Lead species as a function of the initial pH. As it is seen, the species Pb^{2+}, $Pb(OH)_2$ and $Pb(OH)^+$ are formed in pH close to 6. Also, possibility of formation of species $Pb(OH)^{3-}$ and $Pb(OH)^{2-}$ increases in pH values between7 to12. The formation of these common species is due to increasing the concentration of $(OH)^-$ by increasing the amount of pH

[28]. So to avoid formation of these common precipitation and inappropriate interpretation of adsorption, the removal of Lead cation was studied in the acidic pH range (1-6). pH of solutions was adjusted by using HNO_3 and KOH solutions (0.01 M). After adsorption experiments in the same conditions (initial concentration 200ppm; contact time 20 min and adsorbent dosage 0.065 gr), the residual concentration of Lead in solutions was determined and the removal efficiency graph based on the initial pH was plotted (**Fig.4.b**).

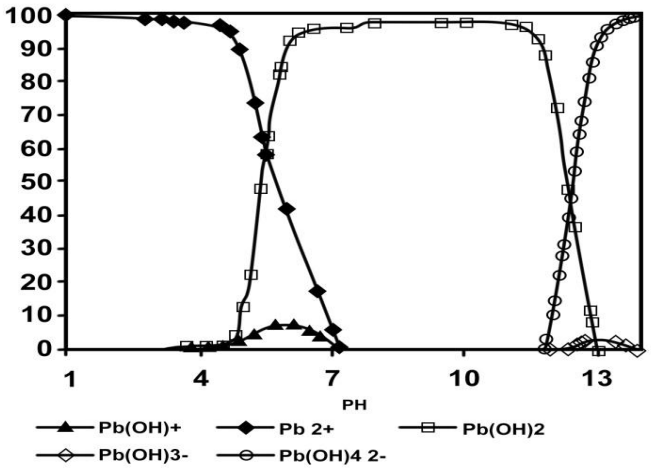

Fig.4.a.The percentage of formed Lead species as a function of the initial pH

According to **Fig.4.b**, when the pH value increases the removal efficiency is also increased. In the pH range 5 to 6, the removal efficiency is reached to maximum value of it (74.9 %). Since increasing in the pH value from 5.75 to 6 has not made significant difference in the removal efficiency value, pH 5.75 was considered as optimum pH.

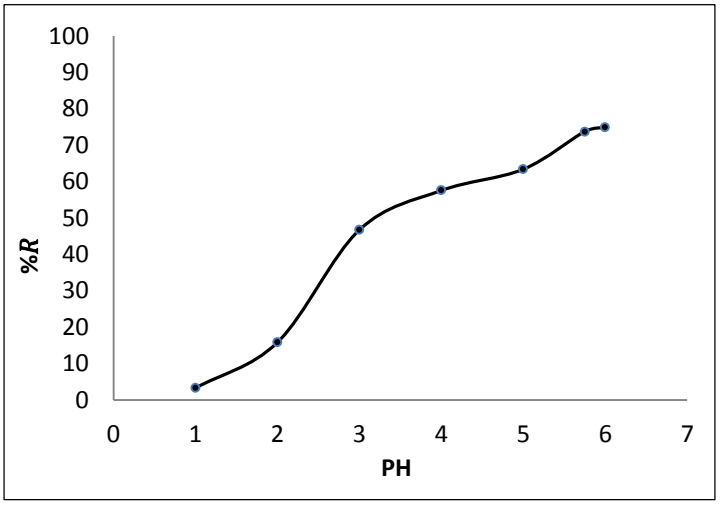

Fig.4.b. The removal efficiency based on the initial pH (initial concentration, 200ppm; contact time, 20 min and adsorbent dosage, 0.065 gr).

Reducing the amount of removal efficiency in the acidic pH range is due to high concentration of H^+ and H_3O^+ in solution which Leads to the occupation of the active ligands of GO/Fe_3O_4/Chi/Cys. When the pH of solution increases, protonation of the functional groups of GO/Fe_3O_4/Chi/Cys surface becomes weaker and provides more ligands for adsorption of Pb^{2+} ions. Besides that, whith increasing pH, electrostatic repulsion between Pb^{2+} ions and negative sites of GO/Fe_3O_4/Chi/Cys becomes stronger; so an increase in the value of the removal efficiency is visible.

3.2.2. EFFECT OF CONTACT TIME

Adsorption behaviors of Pb^{2+} ions were studied in different contact time ranging from 0 min to 180 min and in the fixed initial condition (initial concentration 200ppm; adsorbent dosage 0.065 gr and optimum pH 5.75). The removal efficiency graph as a function of the equilibrium time was plotted in **Fig.5**.

According to Fig.5 after 3 minutes' contact time between adsorbent and Pb^{2+} ions, the removal efficiency increases significantly. This increase may be due to the high concentration gradient of solute and empty active ligands on the adsorbent at the beginning of the reaction. Between 3 to 30 minutes the removal efficiency with lesser sloping than before increases because the number of adsorption sites decreases with increasing contact time. As it can be seen after 30 minutes, the removal efficiency remains almost constant (~ 81%). Since the increase in contact time after 30 minutes, did not have much effect on the

percentage of removal efficiency, the equilibrium time of 30 minutes was considered as optimum time. In other words, adsorption sites in GO/Fe_3O_4/Chi/Cys are completely saturated after 30 minutes so they are not able to remove further.

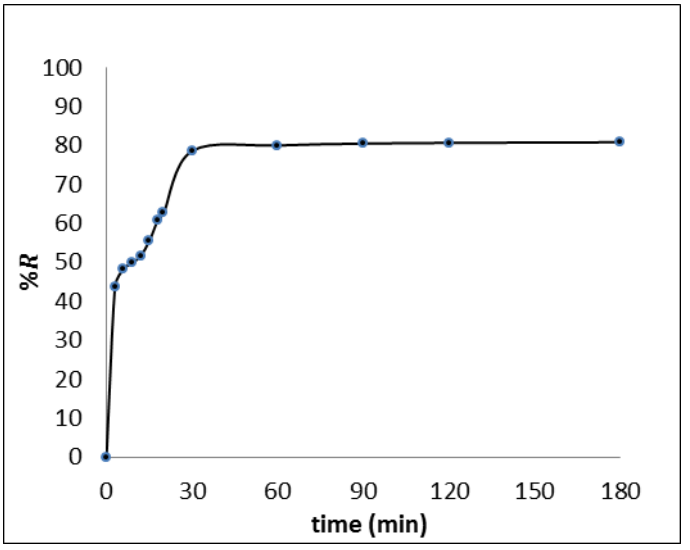

Fig.5. The removal efficiency graph as a function of the equilibrium time (initial concentration, 200ppm; adsorbent dosage, 0.065 gr and $pH_{optimum}$, 5.75).

3.2.3. EFFECT OF ADSORBENT DOSAGE

To determine the optimum adsorbent dosage or the least amount of adsorbent that has the highest removal efficiency, the adsorption experiments were happened in fixed conditions (initial concentration 200ppm; optimum pH 5.75 and optimum contact time 30 min). The effect of adsorbent dosage on the removal efficiency is shown in **Fig.6**.

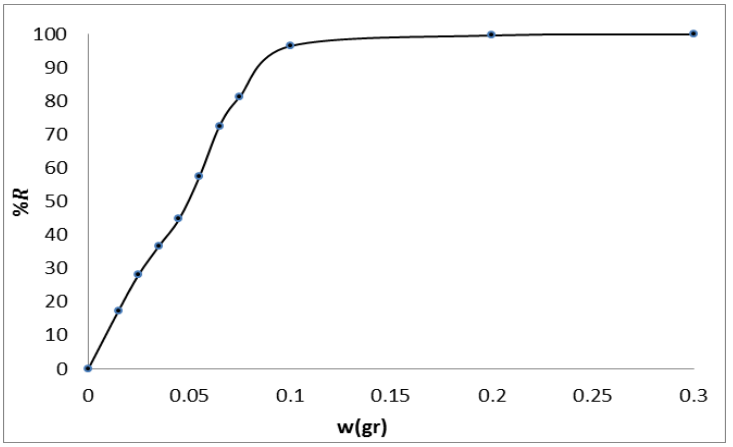

Fig.6. The removal efficiency based on the adsorbent dosage (initial concentration, 200ppm; $pH_{optimum}$, 5.75 and $t_{optimum}$, 30min).

According to Fig.6 at the beginning, a direct relationship exists between increasing amount of GO/Fe_3O_4/Chi/Cys and the removal efficiency; because with increasing amount of GO/Fe_3O_4/Chi/Cys the number of non-saturated and active sites of adsorbent increases and the probability of interaction increases between Pb^{2+} ions with surface. Since the maximum value of removal efficiency (96.5 %) takes place in 0.1gr adsorbent, 0.1 gr was considered as the optimum adsorbent dosage. In quantities above 0.1 gr, increasing the amount of adsorbent has not significant impact on the removal efficiency so it will not be economical in large scale.

3.2.4. Effect of initial concentration of Pb^{2+}

In order to determine the equilibrium concentrations and the maximum adsorption capacity of GO/Fe_3O_4/Chi/Cys in experimental mode (q_{exp}), the effect of initial concentration of Pb^{2+} in the range from10_400 ppm on the removal efficiency and the adsorption capacity was investigated. All experiments were carried out under conditions where the pH value, contact time and the adsorbent dosage were optimized. The results are reported in figures 7.a and 7.b.

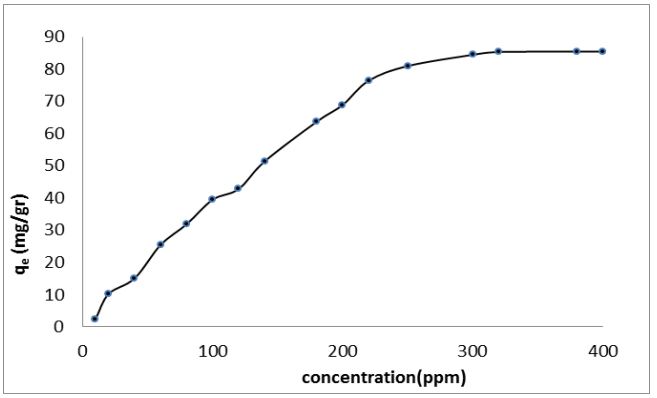

Fig.7.a. The adsorption capacity based on initial metal concentration ($t_{optimum}$, 30min; $pH_{optimum}$, 5.75 and adsorbent dosage, 0.1 gr).

Fig.7.a. shows the relationship between the initial concentration of Pb^{2+} ions and the adsorption capacity. According to this chart, in the first step (10_300 ppm) increasing the initial ions concentration has caused an increase in the q_e value. Because when the number of the ions in the competition to react with surface ligands increases, the numbers of collision between Pb^{2+} ions and active sites of adsorbent increases too. Therefore, the amount of Pb^{2+} adsorbed per unit mass of adsorbent increases. At higher initial concentration (>300 ppm), the q_e value remains constant which may be due to the saturation of active sites of GO/Fe_3O_4/Chi/Cys. So the value of 85.4 mg/gr was considered as the maximum empirical adsorption capacity (q_{exp}) of GO/Fe_3O_4/Chi/Cys.

Fig.7.b. was plotted to determine equilibrium concentrations. The results show that there is a complete removal (100%) at lower initial metal concentration (in the range from 10 to 120ppm); consequently, there is no certainty for the achieving of equilibrium in adsorption. But at concentrations higher than 120 ppm, the removal efficiency is no 100% and it decreases. In other words, the concentration of Pb^{2+} ions in bulk solutions is in a dynamic equilibrium with concentration at the boundary.

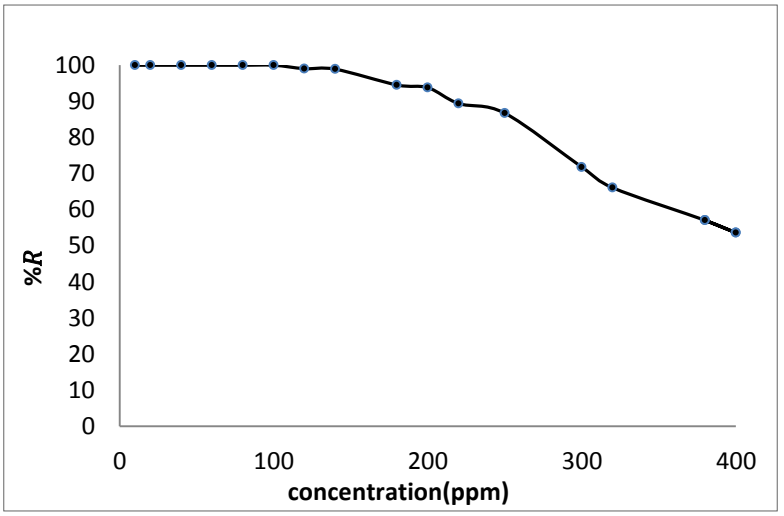

Fig.7.b. The removal efficiency based on the initial metal concentration ($t_{optimum}$, 30min; $pH_{optimum}$, 5.75 and adsorbent dosage, 0.1 gr).

3.2.5. EFFECT OF TEMPERATURE AND THERMODYNAMIC STUDIES

The effect of temperature on the removal efficiency was studied and illustrated in Fig.8. It is obvious that %*R* increased with rising the temperature from 269 to 346 ^{o}K .

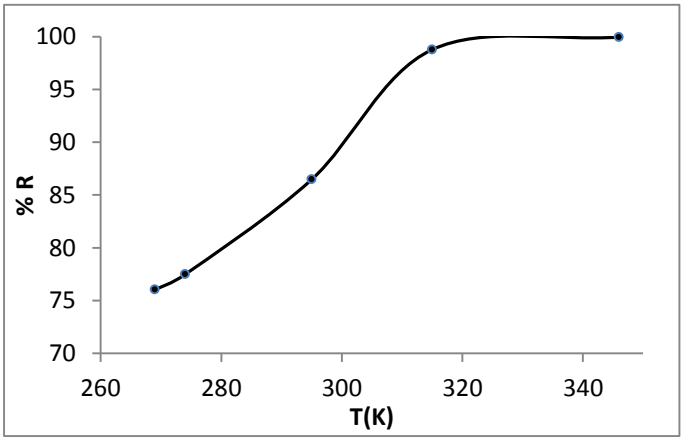

Fig.8. The effect of temperature on the removal efficiency ($t_{optimum}$, 30min; $pH_{optimum}$, 5.75 and adsorbent dosage, 0.1 gr).

The basic thermodynamics conception supposes that the reaction is an isolated system, where the system energy cannot be lost or gained and the only driving force is the entropy change. To investigate more information about the mechanism of the adsorption process, the thermodynamic parameters for the adsorption of lead at different temperatures (269, 274, 295, 315 and 346°K) were calculated using Van't Hoff's equation (Eq. (3)):

$$\ln k = \left(\Delta S^{\circ}/_{R}\right) - \left(\Delta H^{\circ}/_{RT}\right) \quad (3)$$

K is the distribution coefficient at various temperatures and $k = \frac{C_0 - C_e}{C_0} = \frac{a_{ad}}{a_s}$, where a_{ad} and a_e are the activity of adsorbed Pb^{2+} and the activity of Pb^{2+} in solution at equilibrium, respectively. R (8.314 j/mol.k) is the molar gas constant. The average standard enthalpy change (ΔH^{o} in j/mol) and the average standard entropy change (ΔS^{o} in j/k.mol) were calculated from the slope and intercept of the linear plot of lnk versus 1/T, respectively (Fig. 9). The calculated values were tabulated in Table 2. [29]

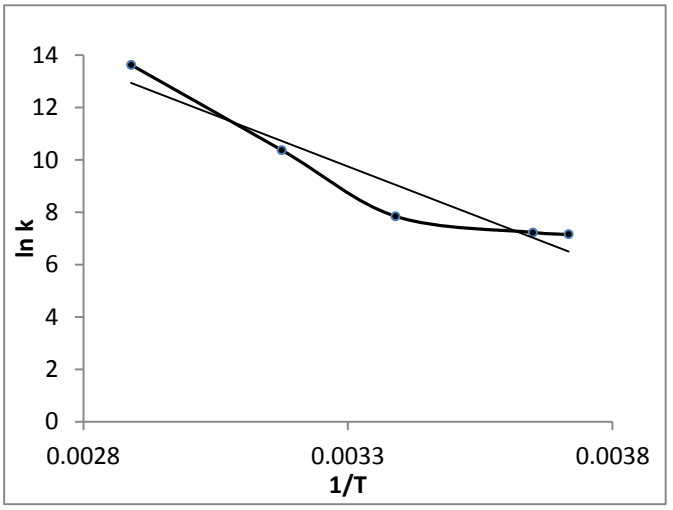

Fig.9. The plot of lnK of Pb^{2+}against 1/T.

Table.2. The thermodynamic parameters for adsorption of Pb^{2+} using GO/Fe3O4/Chi/Cys at different temperature

	ΔH^{o}(j/mol)	ΔS^{o} (j/k.mol)	R^2
Pb^{2+}	64805.97	294.88	0.919

Assuming that enthalpy changes is constant at different temperatures so Standard Gibb's free energies ΔG^{o} (j/mol) were calculated using Eq. (4). (see Table 3)

$$\Delta G^{\circ} = \Delta H^{\circ} - T\Delta S^{\circ} \quad (4)$$

Table.3. Standard Gibb's free energies for adsorption of Pb^{2+} using GO/Fe3O4/Chi/Cys at different temperature

T(^{o}K)	ΔG^{o} (j/mol)
269	-14516.8
274	-15991.2
295	-22183.6
315	-28081.2
346	-37222.5

The negative values of ΔG^{o} indicated that the adsorption process of Pb^{2+} ions onto GO/Fe_3O_4/Chi/Cys is spontaneous in nature. Increasing the temperature leads to an increase in the negativity of ΔG^{o} values for Pb^{2+} and hence, increases the interaction between the GO/Fe_3O_4/Chi/Cys and the metal ions. ΔH^{o} has positive values, indicating that the adsorption process for Pb^{2+} ions was endothermic in nature. Positive values of ΔS^{o} reflect the good affinity of the adsorbent towards the adsorbate ions. Moreover, positive values of ΔS^{o} suggest increasing in randomness state at the solid/solution interface. Solvent molecules displaced by the solute ions, gained extra translational entropy than that lost by the solute ions, therefore allowing the spread of randomness in the system. Also, positive ΔS^{o} values correspond to increasing the degree of freedom of the adsorbed ions.

3.2.6. REUSABILITY

The reusability of GO/Fe_3O_4/Chi/Cys was evaluated by determination of the removal efficiency after several adsorption-desorption cycles as presented in Fig. 10. After five times regeneration, the removal efficiency decreased to 15%, so it can be said that the modified adsorbent can be used as a complementary process for removal of Pb^{2+} ions from water and wastewater.

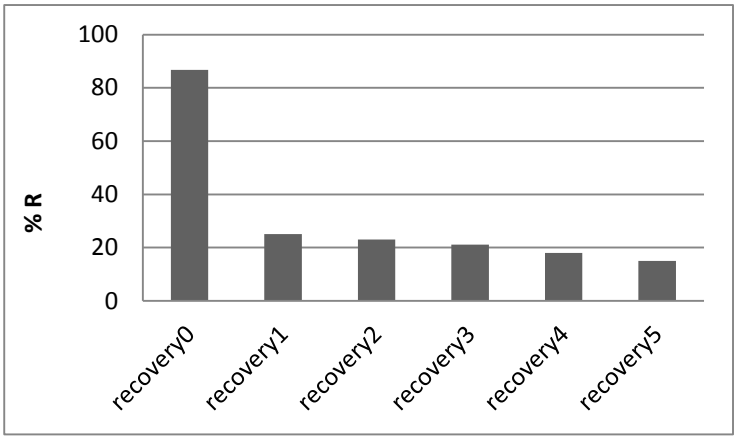

Fig.10. The removal efficiency versus cycle number

4. CONCLUSION

In this paper, a novel adsorbent of GO/Fe_3O_4/Chi/Cys nanocomposite was successfully prepared and investigated for the removal of Lead ions from aqueous solutions. GO/Fe_3O_4/Chi/Cys composites are superparamagnetic at room temperature and can be separated by an external magnetic field. The optimal conditions for adsorption process were achieved at $pH_{Optimum}$=5.75, $t_{Optimum}$=30min and adsorbent dosage=0.1 gr. The maximum adsorption capacity of metal ions calculated for Pb^{2+} was 85.4 mg/gr. Thermodynamic analysis showed that the adsorption process is exothermic and spontaneous in nature. Regeneration studies proved that the prepared adsorbent have the ability to be reused as a complementary process.

ACKNOWLEDGMENTS

This research work was supported by the Islamic Azad University, Marvdasht, Iran.

REFERENCES

[1] H. Ramezani, M. Sharif and A.K Shokooh. *Graphene-Based Polymer Nanocomposites.* Polymerization Quarterly. (2015) 86–107. Available:http://basparesh.ippi.ac.ir/article_1149_dca2849d5ace80b3351429fbf19a064e.pdf

[2] M. Khazaei, S. Nasseri, M.R. Ganjali, M. Khoobi, R. Nabizadeh, E. Gholibegloo and S. Nazmara. *Selective Removal of Lead Ions from Aqueous Solutions using 1, 8-Dihydroxyanthraquinone (DHAQ) Functionalized*

Graphene Oxide; Isotherm, Kinetic and Thermodynamic Studies. RSC Advances. 8(11) (2018)5685-5694.
Available: https://pubs.rsc.org/en/content/articlehtml/2018/ra/c7ra13603j

[3] R. Seenivasan, W.J. Chang and S. Gunasekaran. *Highly Sensitive Detection and Removal of Lead Ions in Water using Cysteine-Functionalized Graphene Oxide /Polypyrrole Nanocomposite Film Electrode.* ACS applied materials & interfaces.7(29) (2015)15935-15943.
Available: https://pubs.acs.org/doi/abs/10.1021/acsami.5b03904

[4] D.Vilela, J. Parmar, Y. Zeng, Y.Zhao and S. Sánchez. *Graphene-Based Microbots for Toxic Heavy Metal Removal and Recovery from Water*. Nano letters.16(4) (2016) 2860-2866.
Available: https://pubs.acs.org/doi/full/10.1021/acs.nanolett.6b00768

[5] D. Mehta, S. Mazumdar and S.K. Singh. *Magnetic Adsorbents for the Treatment of Water/ Wastewater*. Journal of Water Process Engineering. 100(7) (2015) 244-265.
Available:
https://www.sciencedirect.com/science/article/pii/S221471441530026X

[6] H. Rahimi. *Absorption Spectra of a Graphene Embedded One Dimensional Fibonacci Aperiodic Structure.* Journal of Optoelectronical Nanostructures. 3(4) (2018) 45-58
Available: http://jopn.miau.ac.ir/article_3259.html

[7] A. Abdykian and Z. Safi. *Finding Electrostatics Modes in Metal Thin Films by using of Quantum Hydrodynamic Model.* Journal of Optoelectronical Nanostructures.1(3) (2016) 43-50.
Available: http://jopn.miau.ac.ir/article_2193.html

[8] M. Nayeri, P. keshavarzian, M. Nayeri. *A Novel Design of Penternary Inverter Gate Based on Carbon Nano Tube.* Journal of Optoelectronical Nanostructures. 3(1) (2018) 15-26
Available: http://jopn.miau.ac.ir/article_2820.html

[9] K.S. Novoselov, V.I. Fal, L. Colombo, P.R. Gellert, M.G. Schwab and K. Kim. *A Roadmap for Graphene.* Nature.490(7419) (2012)192-200.
Available: https://www.nature.com/articles/nature11458

[10] A. Abdikian, G. Solookinejad, Z. Safi. *Electrostatics Modes in Mono-Layered Graphene.* Journal of Optoelectronical Nanostructures. 1(2) (2016) 1-8.
Available: http://jopn.miau.ac.ir/article_2044.html

[11] D.R. Dreyer, S. Park, C.W. Bielawski and R.S. Ruoff. *The Chemistry of Graphene Oxide.* Chemical Society Reviews.39(1) (2010) 228-240.
Available: https://pubs.rsc.org/en/content/articlehtml/2010/cs/b917103g

[12] D.R. Dreyer, R.S. Ruoff and C.W. Bielawski. *From Conception to Realization: an Historial Account of Graphene and Some Perspectives for its Future.* Angewandte Chemie International Edition.49(49) (2010) 9336-9344.
Available: https://onlinelibrary.wiley.com/doi/abs/10.1002/anie.201003024

[13] S. Pei and H.M. Cheng. *The Reduction of Graphene Oxide.* Carbon.50(9) (2012) 3210-3228.
Available:
https://www.sciencedirect.com/science/article/pii/S0008622311008967

[14] K. Kalantari, M.B. Ahmad, H.R.F. Masoumi, K. Shameli, M. Basri and R. Khandanlou. *Rapid and High Capacity Adsorption of Heavy Metals by Fe_3O_4/Montmorillonite Nanocomposite using Response Surface Methodology: Preparation, Characterization, Optimization, Equilibrium Isotherms, and Adsorption Kinetics Study.* Journal of the Taiwan institute of Chemical Engineers.49 (2015) 192-198.
Available:
https://www.sciencedirect.com/science/article/pii/S1876107014003265

[15] Handbook of Membranes for Industrial Wastewater Recovery and Re-us, 1st ed., Elsevier Science & Technology Books,2003 ,7-9.

[16] T. Kuilla, S. Bhadra, D.Yao, N.H. Kim, S. Bose and J.H. Lee. *Recent Advances in Graphene Based Polymer Composites.* Progress in polymer science.35(11) (2010) 1350-1375.
Available:
https://www.sciencedirect.com/science/article/pii/S0079670010000699

[17] Y.A. El-Reash. *Magnetic Chitosan Modified with Cysteine-Glutaraldehyde as Adsorbent for Removal of Heavy Metals From Water.* Journal of Environmental Chemical Engineering. 4 (4) (2016) 3835-3847.
Available:
https://www.sciencedirect.com/science/article/pii/S2213343716303001

[18] V. Chandra, J. Park, Y. Chun, J.W. Lee, I.C. Hwang and K.S. Kim. *Water-Dispersible Magnetite-Reduced Graphene Oxide Composites for Arsenic Removal.* ACS Nano. 4(7) (2010) 3979-3986.
Available: https://pubs.acs.org/doi/abs/10.1021/nn1008897

[19] S. Tripathi, G.K. Mehrotra and P.K Dutta. *Preparation and Physicochemical Evaluation of Chitosan/poly (vinyl alcohol)/Pectin*

Ternary Film for Food-Packaging Applications. Carbohydrate Polymers.79(3) (2010)711-716.
Available:
https://www.sciencedirect.com/science/article/pii/S0144861709005335

[20] L. Qi and Z. Xu. *Lead Sorption from Aqueous Solutions on Chitosan Nanoparticles*. Colloids and Surfaces A: Physicochemical and Engineering Aspects. 251(1) (2004)183-190.
Available:
https://www.sciencedirect.com/science/article/pii/S0927775704006995

[21] K.A. Janes, M.P. Fresneau, A. Marazuela, A. Fabra and M.J. Chitosan *Nanoparticles as Delivery Systems for Doxorubicin. Alonso*. Journal of controlled Release. 73(2) (2001) 255-267.
Available:
https://www.sciencedirect.com/science/article/pii/S0168365901002942

[22] Y.A. El-Reash. *Magnetic Chitosan Modified with Cysteine-Glutaraldehyde as Adsorbent for Removal of Heavy Metals from Water*. Journal of Environmental Chemical Engineering. 4(4) (2016) 3835-3847.
Available:
https://www.sciencedirect.com/science/article/pii/S2213343716303001

[23] D.D. Lefebvre and C. Edwards, *Decontaminating Heavy Metals from Water using Photosynthetic Microbes*, In Emerging Environmental Technologies, 2 (2009) 57-73.
Available: https://link.springer.com/chapter/10.1007/978-90-481-3352-9_3

[24] R. Wilfried E. *Structure and Function of Metal Chelators Produced by Plants*. Journal of Cell biochemistry and biophysics. 31(1) (1999) 19-48.
Available: https://link.springer.com/article/10.1007/BF02738153

[25] G. Scarano and E. Morelli. *Properties of Phytochelatin-Coated CdS Nanocrystallites Formed in a Marine Phytoplanktonic Alga (Phaeodactylum tricornutum, Bohlin) in response to Cd*. Journal of Plant Science.165(4) (2003) 803-810.
Available:
https://www.sciencedirect.com/science/article/pii/S0168945203002747

[26] M.R. Lasheen, I.Y. El-Sherif., M.E. Tawfik, S.T. El-Wakeel and M.F. El-Shahat. *Preparation and Adsorption Properties of Nano Magnetite Chitosan Films for Heavy Metal Ions from Aqueous Solution*. Journal of Materials Research Bulletin.80 (2016) 344-350.
Available:
https://www.sciencedirect.com/science/article/pii/S0025540816301696

[27] R.A. Khera, M. Iqbal, S. Jabeen, M. Abbas,A. Nazir, J. Nisar, A. Ghaffar, G.A. Shar and M.A. Tahir. *Adsorption Efficiency of Pitpapra under Single and Binary Metal Systems.* Journal of Surfaces and Interfaces.14 (2019)138-145
Available:
https://www.sciencedirect.com/science/article/pii/S2468023018305571

[28] C.P. Poole Jr, F.J. Owens, Introduction to Nanotechnology, in Introduction to Nanotechnology,1st ed.Chicago, 2003.

[29] C.H. Yang.J. *Derivation of the Freundlich Adsorption Isotherm from Kinetics.* Journal of chemical Education.Colloid interface Sci.86(11) (1998) 379-387.
Available: https://pubs.acs.org/doi/abs/10.1021/ed086p1341